Electron acceleration above thunderclouds

Martin Füllekrug, Ivana Kolmasova, Ondřej Santolík, Thomas Farges, József Bór, Alec Bennett, Michel Parrot, William Rison, Ferruccio Zanotti, Enrico Arnone, et al.

HAL Id: insu-01288052
https://insu.hal.science/insu-01288052

Submitted on 14 Mar 2016

Electron acceleration above thunderclouds

Martin Füllekrug[1]**, Ivana Kolmasova**[2]**, Ondrej Santolik**[2,3]**,
Thomas Farges**[4]**, József Bór**[5]**, Alec Bennett**[6]**, Michel Parrot**[7]**,
William Rison**[8]**, Ferruccio Zanotti**[9]**, Enrico Arnone**[10]**,
Andrew Mezentsev**[1]**, Radek Lan**[2]**, Ludek Uhlir**[2]**, Giles Harrison**[11]**,
Serge Soula**[12]**, Oscar van der Velde**[13]**, Jean-Louis Pinçon**[7]**,
Christiane Helling**[14] **and Declan Diver**[15]

[1] Centre for Space and Atmospheric Science, Department of Electronic and Electrical Engineering, University of Bath, Bath, UK
[2] Institute of Atmospheric Physics, Academy of Sciences of the Czech Republic, Prague, Czech Republic
[3] Faculty of Mathematics and Physics, Charles University in Prague, Czech Republic
[4] Commissariat à l'Energie Atomique et aux Energies Alternatives, DAM-DIF, Bruyères le Châtel, France
[5] Research Centre for Astronomy and Earth Sciences, Hungarian Academy of Sciences, Sopron, Hungary
[6] Bristol Industrial and Research Associates Ltd, Portishead, Bristol, UK
[7] Laboratoire de Physique et Chimie de l'Environnement et de l'Espace, CNRS, Orléans, France
[8] New Mexico Tech, Electrical Engineering Department, NM, USA
[9] Italian Meteor and TLE Network, Ferrara, Italy
[10] Istituto di Scienze dell'Atmosfera e del Clima, CNR, Bologna, Italy
[11] Department of Meteorology, University of Reading, Reading, UK
[12] Laboratoire d'Aérologie, Université de Toulouse, CNRS, Toulouse, France
[13] Department of Electrical Engineering, Technical University of Catalonia, Terrassa, Spain
[14] SUPA, School of Physics and Astronomy, University of St Andrews, St Andrews, UK
[15] School of Physics and Astronomy, University of Glasgow, Glasgow, UK

E-mail: eesmf@bath.ac.uk (Martin Füllekrug)

Abstract
The acceleration of electrons results in observable electromagnetic waves which can be used for remote sensing. Here, we make use of ∼4 Hz–66 MHz radio waves emitted by two consecutive intense positive lightning discharges to investigate their impact on the atmosphere above a thundercloud. It is found that the first positive lightning discharge initiates a sprite where electrons are accelerated during the exponential growth and branching of the sprite streamers. This preconditioned plasma above the thundercloud is subsequently exposed to a second positive lightning discharge associated with a bouncing-wave discharge. This discharge process causes a re-brightening of the existing sprite streamers above the thundercloud and initiates a subsequent relativistic electron beam.

Keywords: atmospheric electricity, lightning, electromagnetic wave propagation, storms

1. Introduction

Transient energetic charged particle populations occur in association with thunderstorms where the lightning

electromagnetic field can release electrons from the radiation belts precipitating into the atmosphere (Voss *et al* 1998, 1984). These electrons have typical kinetic energies $\sim$100–250 keV in addition to their rest mass $\sim$511 keV and occur $\sim$0.1–1 s after the causative lightning discharge (Gemelos *et al* 2009). The electrons are decelerated when penetrating the neutral atmosphere and deposit their energy in $\sim$100–2000 km large ionization patches north/south of a lightning discharge in the northern/southern hemisphere (Inan *et al* 2007). Electrons are accelerated to very high energies $\sim$10–100 MeV inside thunderclouds, either in lightning leader tips (Celestin and Pasko 2011) and/or in large scale thunderstorm electric fields (Dwyer and Cummer 2013, Gurevich and Karashtin 2013, Dwyer 2012, Gurevich *et al* 1992). The acceleration of the electrons is accompanied by gamma rays emanating from thunderstorms (Østgaard *et al* 2013, Tavani *et al* 2011, Smith *et al* 2005, Fishman *et al* 1994) which can be used as a diagnostic tool. When the gamma rays interact with air molecules and exceed an energy of $\sim$1.022 MeV, i.e., two times the rest mass of an electron, the gamma rays can disintegrate into an electron–positron pair around $\sim$40–60 km height such that magnetized positrons and electrons are observed on board of satellites in near-Earth space (Briggs *et al* 2011, Carlson *et al* 2009, Dwyer *et al* 2008). Similarly, it was proposed that the lightning electromagnetic field can accelerate electrons above thunderclouds from the cosmic ray layer upwards to produce avalanching relativistic electron beams (Roussel-Dupré *et al* 1998, Roussel-Dupré and Gurevich 1996). Experimental evidence for such electron beams was reported by remote sensing with low frequency radio waves (Füllekrug *et al* 2011b, 2010). The lightning electromagnetic field also causes Joule heating above thunderclouds which results in electrical breakdown of air such that sprite streamers develop (Pasko 2010). The exponential growth and splitting of streamers results in an electron multiplication associated with the acceleration of electrons to a few eV. The accelerated electrons radiate a small amount of electromagnetic energy and the incoherent superposition of many streamers causes low frequency radio noise (Füllekrug *et al* 2013a, Qin *et al* 2012a). As a result, the remote sensing with radio waves can be used to investigate the acceleration of electrons above a thundercloud during a sprite followed by a consecutive electron beam which is the aim of this contribution.

2. Observations

Unstable air masses near the north-eastern coast of Spain developed into a thunderstorm in the evening of 29 August 2012. The storm propagated eastward along the Mediterranean coast of southern France and produced numerous lightning discharges in the early morning hours of August 30. The accumulated leader steps of one particular $\sim$1.7 s long lightning discharge were recorded with a lightning mapping array in 80 μs long time intervals as part of the HyMeX campaign (figure 1). Shortly after the beginning of the discharge process, one particularly intense positive lightning discharge (44.0°N, 5.6°E) with a peak
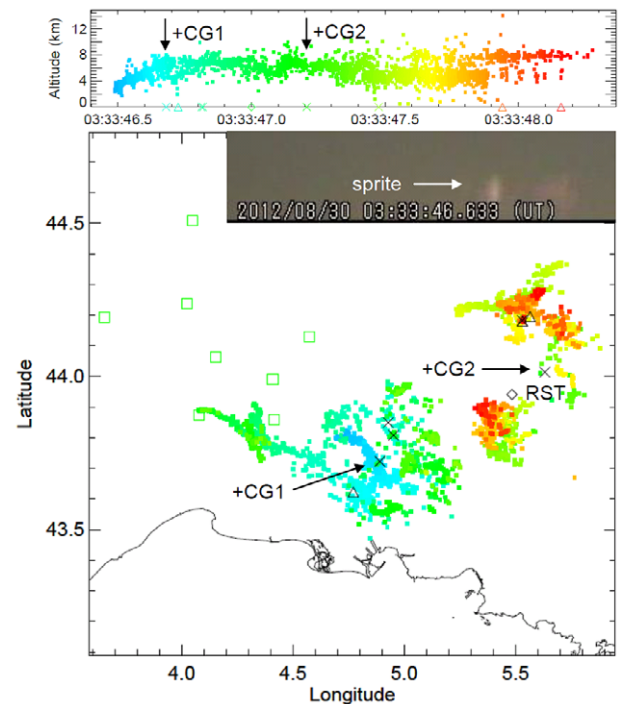

Figure 1. A lightning mapping array (green squares) records the leader steps of a $\sim$1.7 s long lightning discharge on 30 August 2012 (upper panel), which causes numerous positive (crosses) and negative (triangles) cloud to ground lightning discharges. A particularly intense positive cloud to ground lightning discharge at 03:33:46.680 (+CG1) causes a sprite (inset figure). The consecutive intense positive cloud to ground lightning discharge at 03:33:47.208 (+CG2) occurs $\sim$60 km north-eastward of the sprite and is recorded with a high frequency radio receiver near Rustrel (RST).

current of +124 kA occurred at 03:33:46.680 UTC and caused a subsequent sprite. The sprite was recorded with an astronomical color video camera in Ferrara (44.8°N, 11.6°E) as part of the Italian Meteor and TLE network. The sprite producing lightning discharge was associated with a charge moment change as large as $\sim$1300 C km. The charge moment was calculated from an exponentially decreasing lightning current inferred from electric field measurements in the frequency range $\sim$5–30 Hz (figure 2, left, upper panel) at Nagycenk observatory (47.6°N, 16.7°E) in Hungary (Sátori *et al* 2013, and references therein). This large charge moment change exceeded the charge moment change $\sim$600 C km which is typically required for sprite initiation (Qin *et al* 2012b, Cummer *et al* 2005). The lightning discharge was also intense enough to be picked up by a quasi-static current sensor operated in the frequency range of $\sim$1–50 Hz near Portishead (51.5°N, 2.8°W) in south-west England. Similar unusual quasi-static current signatures (figure 2, left, middle panel) have previously been used to successfully detect sprites with $\sim$30–50% detection efficiency because the detected sprites are almost certainly associated with halos (Bennett and Harrison 2013). Finally, the sprite streamers produced low frequency radio noise from $\sim$4–400 kHz (Füllekrug *et al* 2013a, Qin *et al* 2012a) lasting for $\sim$20 ms which was measured here with two independently recording radio receivers near Orléans (47.8°N, 1.9°E) in central France and
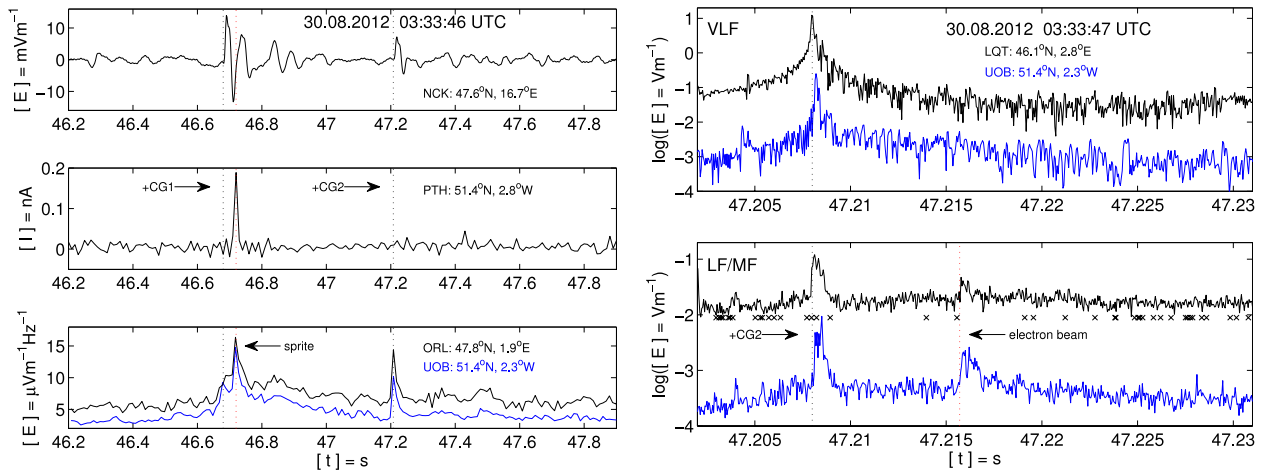
Figure 2. Left. Upper panel. Electric field measurements from ~5–30 Hz at Nagycenk (NCK) are used to infer the charge moment change of the two consecutive lightning discharges (black dotted lines). The charge moment of the first positive lightning discharge exceeds the limit for sprite initiation. The second positive lightning discharge exhibits a much smaller charge moment. Middle panel. The recordings of the quasi-static current from ~1–50 Hz near Portishead (PTH) indicate that the first lightning discharge initiated a sprite. Lower panel. The low frequency radio noise from ~4–400 kHz near Orléans (ORL) and Bath (UOB) indicates radio emissions from sprite streamers (red dotted line) initiated by the first lightning discharge and a re-brightening of the remaining sprite streamers during the second lightning discharge. Right. Upper panel. The second lightning discharge exhibits the typical ~0.1–1 ms long ~5–15 kHz (VLF) electric field enhancement which is larger in LeQuartier (LQT) when compared to Bath as a result of the proximity to the lightning discharge. Lower panel. About ~8–9 ms after the second lightning discharge, a ~1 ms long ~270–400 kHz (LF/MF) radio pulse indicates the acceleration of electrons associated with an electron beam which is recorded by both radio receivers. Note that the leader steps recorded with the lightning mapping array from ~60–66 MHz (crosses in the lower panel) do not seem to be related to the VLF or LF/MF recordings.

Bath (51.4°N, 2.3°W) in south-west England (figure 2, left, lower panel). The remarkable coincidence of three entirely different proxy measures of sprite occurrence (figure 2, left) ensures that the luminosity patch observed with the video camera was indeed a sprite.

The low frequency radio noise from the sprite streamers is followed ~528 ms later by a new intense positive lightning discharge (44.0°N, 5.6°E) with a peak current of ~+121 kA which occurs at 03:33:47.208 UTC. The lightning discharge is located ~60 km north-east of the preceding lightning discharge and it exhibits a ~0.1–1 ms long 5–15 kHz electric field enhancement as recorded by the radio receiver near Bath and a vertical electric dipole antenna located near LeQuartier in central France (46.1°N, 2.8°E), ~200 km north of the lightning discharge (figure 2, right, upper panel). The lightning discharge has a significantly smaller charge moment change of ~570 C km than the preceding lightning discharge (figure 2, left, upper panel) and no quasi-static current is observed (figure 2, left, middle panel). The absence of a large charge moment change and a quasi-static current indicate that no full sprite developed such that the resurgence of the low frequency radio noise strongly suggests a weaker re-brightening of the existent sprite streamers (figure 2, left, lower panel). However, resonance type oscillations with a period of ~3.8 μs (~260 kHz) lasting for ~9 cycles over ~34.2 μs are superimposed on the radio signal from the cloud to ground lightning discharge (figure 3) as observed with high frequency magnetic field recordings from ~5 kHz–40 MHz (Kolmasova and Santolik 2013) near Rustrel (43.9°N, 5.5°E) at a distance of ~40 km north-east of the initial sprite and ~16 km south-west of the second positive lightning discharge. The second positive lightning discharge with the resonance
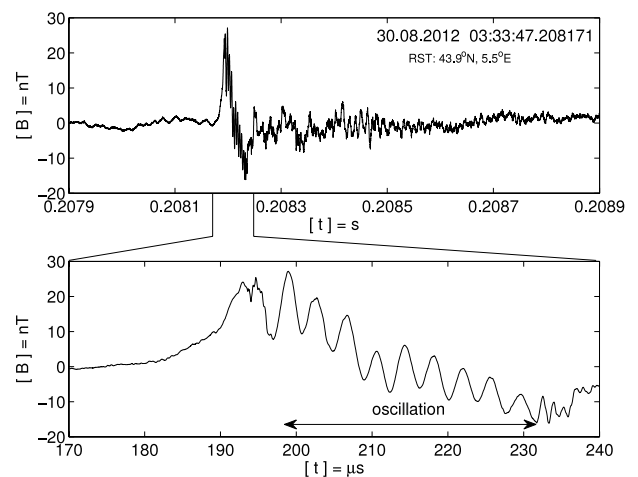

Figure 3. The high frequency magnetic field measurements from ~5 kHz–40 MHz near Rustrel (RST) show that the second positive lightning discharge (upper panel) exhibits resonant type oscillations with a period of ~3.8 μs (~260 kHz) lasting for ~9 cycles over ~34.2 μs (lower panel) attributed to a bouncing-wave discharge.

type oscillations is followed ~8–9 ms later by a characteristic ~1 ms long ~270–400 kHz radio pulse recorded by the radio receivers near Bath and LeQuartier (figure 2, right, lower panel). This radio pulse has a relatively featureless flat spectrum extending from ~40–300 kHz when compared to the spectrum of ordinary lightning discharges (Füllekrug *et al* 2011b) which typically exhibit larger amplitudes at lower frequencies with a relative maximum near ~10 kHz (figure 2, right, upper panel). A more detailed analysis of the electric field recordings in LeQuartier shows that the spectrum of the radio pulse extends up to ~400–500 kHz,

but the presence of medium wave radio transmitters from ∼500–1600 kHz and the local electromagnetic environment inhibit an unambiguous assertion on the extent of the spectrum towards higher frequencies.

3. Interpretation

The first intense positive lightning discharge causes a sprite as evidenced by the optical observations and the radio recordings. The lightning discharge is followed ∼528 ms later by a second positive lightning discharge which exhibits ∼34.2 μs long resonance type oscillations at ∼260 kHz. This second lightning discharge is followed ∼8–9 ms later by a ∼1 ms long ∼270–400 kHz radio pulse.

This pulsed discharge event was initially discovered by high frequency magnetic field recordings with a ground based doublet of a high frequency receiver (Kolmasova and Santolik 2013) which is being developed for the TARANIS spacecraft (Blanc *et al* 2007). It was the only high frequency event recorded during the passage of the thunderstorm. The high frequency recordings of the second lightning discharge exhibit resonance type oscillations with a period of ∼3.8 μs lasting for about ∼34.2 μs. These oscillations are superimposed on the radio signal from the lightning discharge. To the best of our knowledge, these type of oscillations have been observed and reported only in connection with compact intracloud discharges (Nag and Rakov 2009). However, in our case the observed lightning discharge lacks some typical features of compact intracloud discharges. The bouncing wave can be explained by a traveling current pulse which is injected at one end of a conducting channel and reflected multiple times at both ends of the channel until the instability is attenuated and absorbed (Nag and Rakov 2009). The modeling results for the current propagation and reflection show that the pulse travels at a speed between ∼10^8 m s^{-1} and the speed of light (Nag *et al* 2010). In this case, the length of the lightning channel would be ∼1 km resulting in the lower charge moment which is still consistent with a large peak current of the lightning discharge.

The bouncing-wave discharge is followed ∼8–9 ms later by a ∼1 ms long ∼270–400 kHz radio pulse without corresponding radio emissions near ∼10 kHz which are typical for ordinary lightning discharges (figure 2, right, upper panel). The radio pulse is also not associated with radio emissions near ∼60–66 MHz from intracloud lightning discharges (figure 2, right lower panel). The absence of ∼10 kHz radio emissions during the radio pulse also excludes an interpretation of the radio pulse as resurgent impulsive radio noise emanating from sprite streamers which exhibit a spectrum with amplitudes which increase towards lower frequencies (Füllekrug *et al* 2013a). On the other hand, the radio pulse was clearly observed by two entirely independent radio recordings, i.e., with the dipole antenna in LeQuartier and the flat plate antenna in Bath. Radio signatures with the observed characteristics have been predicted by numerical simulations of relativistic runaway breakdown above thunderclouds (Roussel-Dupré *et al* 1998, Roussel-Dupré and Gurevich 1996). These theoretical predictions
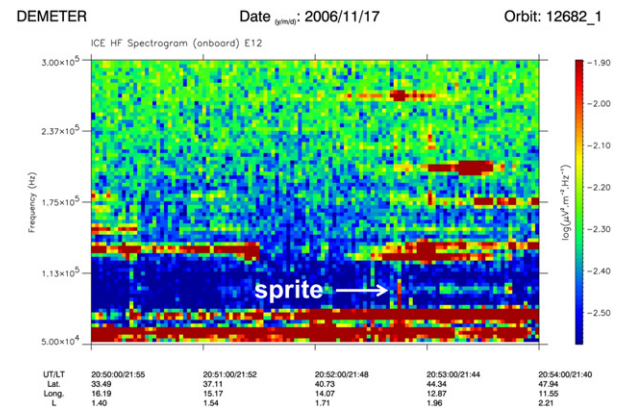

Figure 4. A sprite producing lightning discharge emits a particularly intense broadband radio signal up to ∼130 kHz which was recorded on board the DEMETER spacecraft on 17 November 2006.

have recently been confirmed by experimental measurements (Füllekrug *et al* 2011b, 2010). It is shown here for the first time that such experimental observations cannot easily be explained by currently known lightning discharge processes and that corresponding measurements can be obtained by another radio receiver with a sufficient sensitivity. As a result, the observed radio pulse is attributed to a relativistic electron beam following a sprite producing lightning discharge as predicted by numerical model simulations.

It is interesting to note that a recent detailed comparison of ground based optical sprite observations in southern France with electric field recordings on board the DEMETER satellite on 17 November 2006 (Parrot *et al* 2013), revealed low frequency radio signals up to ∼130 kHz associated with the sprite and/or the causative lightning discharge which have never been observed before in association with ordinary lightning discharges (figure 4). Given that the ionosphere attenuates ∼100 kHz radio signals by ∼2 orders of magnitude (Füllekrug *et al* 2011a), the signal intensity of the lightning and/or sprite was undoubtedly exceptionally large. This observation shows that powerful low frequency radio signals associated with sprite producing lightning, as reported here, can be observed in space with unprecedented temporal and spectral resolution which is the aim of the French TARANIS satellite due to be launched in 2015 (Blanc *et al* 2007).

4. Discussion

In plasma physics it is known that pulsed discharges can accelerate and beam electrons efficiently in the presence of a specific electrostatic field configuration defined by a hollow cathode (Becker *et al* 2006, Slevin and Harrison 1975). It is speculated that a similar physical mechanism might occur above thunderclouds in the presence of aerosols (Füllekrug *et al* 2013b, pp 8–9). In this picture, the first lightning discharge produces free electrons which attach to the aerosols and cause a quasi-static electric field. This electric field defines the geometric shape and the physical properties of any consecutive discharge process. For example, the leader
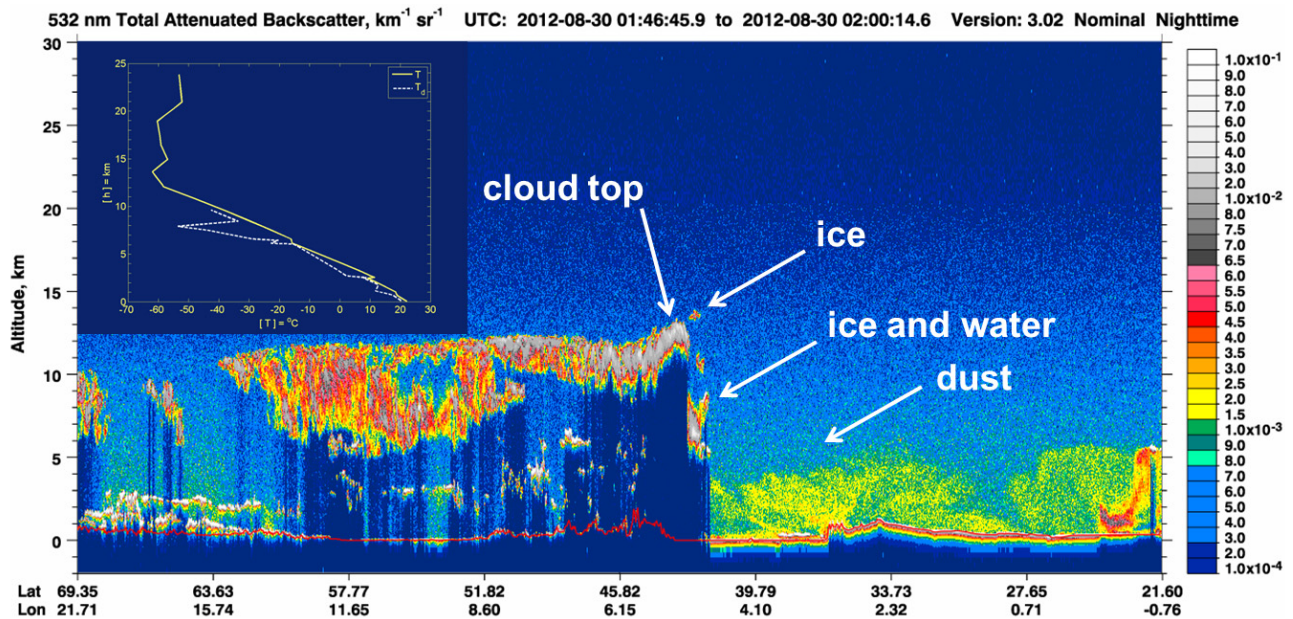
Figure 5. The thunderstorm cloud top height reaches up to ∼12–13 km as inferred from lidar measurements on board the CALIPSO spacecraft. Above the maximum cloud top height, an ensemble of stratospheric ice particles occurs at ∼13–14 km around the tropopause as inferred from temperature measurements during a preceding radiosonde ascent (inset figure). The mixed phase region of the thundercloud is found at ∼6–7 km height where ice and water coexist. The convective storm might have entrained dust which is confined to a layer from the ground up to ∼5–6 km.

stem of a gigantic jet defined the shape of a consecutive ring-formed column sprite (Neubert *et al* 2011, figure 1). The mechanism proposed here requires knowledge on the presence of charged aerosols above thunderclouds. The recent discovery of sporadic stratospheric aerosol layers (Renard *et al* 2010) which are possibly charged (Renard *et al* 2013) suggests that the presence of small quantities of stratospheric aerosols could assist the occasional formation of relativistic electron beams above thunderclouds caused by consecutive lightning discharges. In the absence of *in situ* measurements of charged aerosols above the thunderclouds investigated here, it is interesting to put the electromagnetic observations in the context of the surrounding atmospheric environment.

Air masses from a Saharan dust storm reached France around 17 August 2012, which might have helped to entrain silt into convective storms. The size of silt particles ranges from ∼2–4 μm to ∼62–64 μm and they tend to be larger than clay and smaller than sand. Silt can be carried over long distances in air, whereas sand particles settle down more quickly as a result of gravitational forces and clay particles attach more quickly to any larger particles. Interestingly, Saharan dust storms can be electrified (Nicoll *et al* 2011) such that dust particles are aligned by the electric field (Ulanowski *et al* 2007). In addition, smoke particles from ongoing forest fires in Spain might have been transported by the westerly trade winds towards air masses in France during the month of August and an unusual large number of sprites was observed in the second half of August 2012 as reported by numerous observers on the Eurosprite mailing list. It was previously speculated that the presence of smoke particles can increase the occurrence rate of positive lightning discharges inside

thunderstorms and thereby increase the occurrence rate of sprites above thunderstorms (Lyons, *et al* 1998).

The CALIPSO spacecraft (Cloud–Aerosol Lidar and Infrared Pathfinder Satellite Observation) passed over the investigated thunderstorm around ∼01:53 UTC and determined a thunderstorm cloud top height of ∼12–13 km (figure 5). These large heights are required for compact intracloud discharges to occur. In addition, CALIPSO reported the presence of a dust layer from the ground up to ∼5–6 km height (figure 5). It is very likely that this dust was entrained into the convective storm and transported upwards to the tropopause by convective updrafts. The tropopause was located around ∼13–14 km height as inferred from the radiosonde ascent from Nimes-Courbessac (43.9°N, 4.4°E) at 00:00 UTC (figure 5, inset). Finally, CALIPSO detected a disconnected ensemble of ice particles at ∼13–14 km height which might have been injected into the lower stratosphere by an overshooting cloud top where dust and smoke particles assisted ice nucleation. In any case, the unusual accumulation of ice particles above the thundercloud top might have helped to define a particular electrostatic charge configuration leading to the bouncing-wave discharge and/or the subsequent electron beam.

5. Summary

The impact of two consecutive positive lightning discharges on the area above a thundercloud is investigated in detail. It is found that the first positive lightning discharge initiates sprite streamers which discharge the lightning electromagnetic field above the thundercloud. The exponential growth and

splitting of the streamers results in an electron multiplication associated with the acceleration of electrons to a few eV. A consecutive positive lightning discharge occurs ∼528 ms later and is associated with a bouncing-wave discharge. About ∼8–9 ms after the bouncing-wave discharge an electron beam occurs associated with the acceleration of electrons to a few MeV. This is the first simultaneous detection of radio signatures from electrons accelerated to thermal and relativistic energies above thunderclouds. The environmental conditions leading to the bouncing-wave discharge and the subsequent electron beam remain to be investigated in more detailed future studies.

Acknowledgments

References

Becker K, Schoenbach K and Eden J 2006 *J. Phys. D: Appl. Phys* **39** R55–70

Bennett A and Harrison R 2013 *Phys. Rev. Lett.* **111** 045003

Blanc E, Lefeuvre F, Roussel-Dupré R and Sauvaud J 2007 *Adv. Space Res.* **40** 1268–75

Briggs M *et al* 2011 *Geophys. Res. Lett.* **38** L02808

Carlson B, Lehtinen N and Inan U 2009 *Coupling of Thunderstorms and Lightning Discharges to Near-Earth Space* ed N Crosby, T Huang and M Rycroft (Melville, NY: American Institute of Physics) pp 84–91

Celestin S and Pasko V 2011 *J. Geophys. Res.* **116** A03315

Cummer S, Zhai Y, Hu W, Smith D, Lopez L and Stanley M 2005 *Geophys. Res. Lett.* **32** L08811

Dwyer J 2012 *J. Geophys. Res.* **117** A02308

Dwyer J and Cummer S 2013 *J. Geophys. Res.* **118** 3769–90

Dwyer J, Grefenstette B and Smith D 2008 *Geophys. Res. Lett.* **35** L02815

Fishman G *et al* 1994 *Science* **264** 1313–6

Füllekrug M, Hanuise C and Parrot M 2011a *Atmos. Chem. Phys.* **11** 667–73

Füllekrug M, Mezentsev A, Soula S, van der Velde O and Farges T 2013a *Geophys. Res. Lett.* **40** 2395–9

Füllekrug M, Roussel-Dupré R, Symbalisty M, Chanrion O, Odzimek A, van der Velde O and Neubert T 2010 *J. Geophys. Res.* **115** A00E09

Füllekrug M *et al* 2011b *Atmos. Chem. Phys.* **11** 7747–54

Füllekrug M *et al* 2013b *Surv. Geophys.* **34** 1–41

Gemelos E, Inan U, Walt M, Parrot M and Sauvaud J 2009 *Geophys. Res. Lett.* **36** L21107

Gurevich A and Karashtin A 2013 *Phys. Rev. Lett.* **110** 185005

Gurevich A, Milikh G and Roussel-Dupré R 1992 *Phys. Lett.* A **165** 463–8

Inan U, Piddyachiy D, Peter W, Sauvaud J and Parrot M 2007 *Geophys. Res. Lett.* **34** L07103

Kolmasova I and Santolik O 2013 *Geophys. Res. Lett.* **40** 1637–41

Lyons W, Nelson T, Williams E, Cramer J and Turner T 1998 *Science* **282** 77

Nag A and Rakov V 2009 *IEEE Trans. Electromagn. Compat.* **51** 466–70

Nag A, Rakov V, Tsalikis D and Cramer J 2010 *J. Geophys. Res.* **115** D14115

Neubert T, Chanrion O, Arnone E, Zanotti F, Cummer S, Füllekrug M, Soula S and van der Velde O 2011 *J. Geophys. Res.* **116** A12329

Nicoll K, Harrison R and Ulanowski Z 2011 *Environ. Res. Lett.* **6** 014001

Østgaard N, Gjesteland T, Carlson B, Collier A, Cummer S, Lu G and Christian H 2013 *Geophys. Res. Lett.* **40** 2423–6

Parrot M, Sauvaud J, Soula S, Pincon J and van der Velde O 2013 *J. Geophys. Res.* at press

Pasko V 2010 *J. Geophys. Res.* **115** A00E09

Qin J, Celestin S and Pasko V 2012a *Geophys. Res. Lett.* **39** L22803

Qin J, Celestin S and Pasko V 2012b *Geophys. Res. Lett.* **39** L22801

Renard J, Berthet G, Salazar V, Catoire V, Tagger M, Gaubicher B and Claude R 2010 *Geophys. Res. Lett.* **37** L20803

Renard J, Tripathi S, Michael M, Rawal A, Berthet G, Füllekrug M, Harrison R, Robert C, Tagger M and Gaubicher B 2013 *Atmos. Chem. Phys. Discuss.* **13** 7061–79

Roussel-Dupré R and Gurevich A 1996 *J. Geophys. Res.* **101** 2297–311

Roussel-Dupré R, Symbalisty E, Taranenko Y and Yukhimuk V 1998 *J. Atmos. Sol.-Terr. Phys.* **60** 917–40

Sátori G, Rycroft M, Bencze P, Märcz F, Bór J, Barta V, Nagy T and Kovács K 2013 *Surv. Geophys.* **34** 255–92

Slevin P and Harrison W 1975 *Appl. Spectrosc. Rev.* **10** 201–55

Smith D, Lopez L, Lin R and Barrington-Leigh C 2005 *Science* **307** 1085–8

Tavani M *et al* 2011 *Phys. Rev. Lett.* **106** 018501

Ulanowski Z, Bailey J, Lucas P, Hough J and Hirst E 2007 *Atmos. Chem. Phys.* **7** 6161–73

Voss H, Walt M, Imhof W, Mobilia J and Inan U 1984 *Nature* **312** 740–2

Voss H, Walt M, Imhof W, Mobilia J and Inan U 1998 *J. Geophys. Res.* **103** 11725–44